Electronic Supplementary Material (ESI) for Physical Chemistry Chemical Physics.

Reaction Mechanism Conversion Induced by Contest of Nucleophile and Leaving Group

Siwei Zhao,[a] Gang Fu,[a] Wenqing Zhen,[a] Li Yang,[a,b,*] Jianmin Sun,[a,c,*] and Jiaxu Zhang[a,b,*]

[a] MIIT Key Laboratory of Critical Materials Technology for New Energy Conversion and Storage, School of Chemistry and Chemical Engineering,

[b] State Key Lab of Advanced Welding and Joining,

[c] State Key Lab of Urban Water Resource and Environment,

Harbin Institute of Technology,

Harbin 150001, P. R. China

Author E-mail Address: yangli2014@hit.edu.cn, sunjm@hit.edu.cn, and zhjx@hit.edu.cn

Table S1. Geometries of the OH^- + CH_3Cl stationary points.

	MP2	B3LYP	M06	B97-1	BhandH	CCSD(T)-F12b[a]	Expt[b]
				OH^-			
$R_{O–H1}$	0.973	0.970	0.963	0.969	0.958		
				CH_3Cl			
$R_{C–Cl}$	1.797	1.810	1.794	1.809	1.767		1.785
$R_{C–H2}$	1.096	1.094	1.094	1.095	1.090		1.090
$\theta_{H2\text{-}C\text{-}H3}$	110.7	110.9	110.6	111.0	110.4		110.8
				$[HOH\cdot\cdot CH_2Cl]^-$ (TS0)			
$R_{C–Cl}$	1.806	1.827	1.821	1.825	1.779	1.786	
$R_{C–H2}$	2.012	1.994	2.038	1.988	1.933	2.047	
$\theta_{C\text{-}H2\text{-}O}$	167.0	173.5	164.5	171.2	163.3	163.7	
				$OH^-\cdots HCH_2Cl$ (im1)			
$R_{C–H2}$	1.124	1.141	1.149	1.152	1.161	1.126	
$R_{C–Cl}$	1.830	1.857	1.843	1.854	1.806	1.974	
$R_{O–H2}$	1.769	1.713	1.683	1.679	1.573	1.717	
$R_{O–H1}$	0.970	0.967	0.961	0.966	0.956	0.962	
$R_{C–H3}$	1.098	1.096	1.098	1.099	1.094	1.087	
$\theta_{H2\text{-}C\text{-}Cl}$	110.5	111.6	111.6	111.3	110.4	109.6	
$\theta_{C\text{-}H2\text{-}O}$	158.7	162.6	164.8	165.0	170.2	164.4	
$\theta_{H1\text{-}O\text{-}H2}$	136.6	117.4	115.7	114.3	117.2	122.7	
				$[OH\cdot\cdot HCH_2\cdot\cdot Cl]^-$ (TS1)			
$R_{C–H2}$	1.094	1.094	1.100	1.096	1.090	1.084	
$R_{C–Cl}$	1.840	1.883	1.865	1.878	1.816	1.824	
$R_{C–H3}$	1.093	1.091	1.093	1.093	1.087	1.082	
$R_{O–H2}$	2.074	2.055	1.975	2.050	1.996	2.056	
$R_{O–H1}$	0.971	0.968	0.961	0.967	0.956	0.963	
$\theta_{H2\text{-}C\text{-}Cl}$	110.5	111.2	112.9	111.5	111.4	110.9	
$\theta_{C\text{-}H2\text{-}O}$	112.4	115.1	118.0	115.4	107.6	112.8	

			$OH^{-}\cdots CH_3Cl$ (im1')			
R_{C-O}	2.614				2.489	2.600
R_{C-Cl}	1.850				1.827	1.834
R_{O-H1}	0.971				0.956	0.963
R_{C-H2}	1.091				1.085	1.081
θ_{O-C-Cl}	169.3				168.6	168.6
θ_{C-O-H1}	158.5				152.5	154.6
			$[OH\cdot\cdot CH_3\cdot\cdot Cl]^{-}$ (TS1')			
R_{C-O}	2.237				2.212	2.227
R_{O-H1}	0.972				0.957	0.964
R_{C-H3}	1.084				1.079	1.072
R_{C-Cl}	2.056				1.998	2.053
θ_{C-O-H1}	110.1				112.8	107.8
θ_{H2-C-O}	76.6				75.2	77.1
$\theta_{H2-C-Cl}$	99.7				101.4	99.8
			$CH_3OH\cdots Cl^{-}$ (im2)			
R_{C-O}	1.420	1.409	1.394	1.407	1.379	1.405
R_{C-H2}	1.103	1.103	1.103	1.104	1.099	1.094
R_{O-H1}	0.993	0.995	0.990	0.994	0.987	0.985
R_{H1-Cl}	2.104	2.101	2.121	2.095	2.011	2.097
θ_{C-O-H1}	104.9	107.1	106.0	106.5	106.4	105.4
$\theta_{O-H1-Cl}$	166.8	171.5	165.1	170.5	166.2	166.8
θ_{H3-C-O}	112.0	112.3	112.6	112.3	112.3	112.0
			$[OH\cdot\cdot H\cdot\cdot CH_2Cl]^{-}$ (TS2)			
R_{O-H1}	0.968	0.966	0.961	0.965	0.956	
R_{O-H2}	1.152	1.203	1.303	1.219	1.218	
R_{C-H2}	1.507	1.440	1.326	1.417	1.383	
R_{C-Cl}	1.885	1.910	1.876	1.899	1.838	
θ_{O-H2-C}	179.3	176.8	178.6	177.2	179.4	

$\theta_{H2\text{-}C\text{-}Cl}$	107.8	111.1	108.9	110.6	108.9		
				HOH···CH_2Cl^- (im3)			
$R_{O–H1}$	0.967	0.964	0.960	0.964	0.955		
$R_{O–H2}$	1.064	1.058	1.020	1.058	1.047		
$R_{C–H2}$	1.691	1.718	1.837	1.707	1.675		
$R_{C–Cl}$	1.904	1.946	1.939	1.934	1.869		
$\theta_{O\text{-}H2\text{-}C}$	174.9	178.1	168.3	177.2	171.8		
$\theta_{H2\text{-}C\text{-}Cl}$	104.1	108.9	98.6	107.8	102.0		
				[OH··CH_3··Cl]$^-$ (TS3)			
$R_{C–Cl}$	2.215	2.341	2.294	2.309	2.186	2.263	
$R_{C–O}$	2.048	2.170	2.110	2.136	1.984	2.080	
$R_{O–H1}$	0.976	0.972	0.966	0.971	0.961	0.968	
$\theta_{O\text{-}C\text{-}Cl}$	80.7	81.5	80.8	81.2	80.7	80.7	
$\theta_{H1\text{-}O\text{-}C}$	92.8	93.1	94.5	93.3	96.4	92.4	
				CH_3OH			
$R_{C–O}$	1.435	1.427	1.410	1.424	1.394		1.425
$R_{C–H2}$	1.103	1.097	1.097	1.098	1.093		1.094
$R_{O–H1}$	0.966	0.964	0.961	0.963	0.954		0.945
$\theta_{C\text{-}O\text{-}H1}$	107.9	108.9	109.1	108.5	109.8		108.5
$\theta_{H2\text{-}C\text{-}H3}$	108.7	108.5	108.0	108.4	108.0		108.6
				H_2O			
$R_{O–H2}$	0.966	0.965	0.961	0.964	0.955		0.958
$\theta_{H1\text{-}O\text{-}H2}$	103.9	104.7	104.7	104.4	105.6		104.5
				CH_2Cl^-			
$R_{C–H3}$	1.119	1.117	1.118	1.120	1.108		
$R_{C–Cl}$	1.936	1.993	1.974	1.977	1.898		
$\theta_{H3\text{-}C\text{-}Cl}$	99.4	97.9	97.9	98.0	99.9		

[a]The geometries of the stationary points at CCSD(T)-F12b/aug-cc-pVTZ level in ref 31; [b]The experimental geometries for reactants and products in ref 42; Bond lengths are

in angstroms (Å), and angles are in degree.

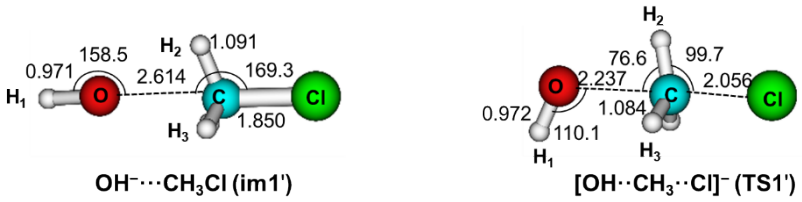

Figure S1. Structures of $OH^{-}\cdots CH_3Cl$ (im1') and $[OH\cdot\cdot CH_3\cdot\cdot Cl]^{-}$ (TS1') for the OH^{-} + CH_3Cl reaction at MP2/aug-cc-pVDZ level.

Table S2. Average Fractions of $OH^- + CH_3Y \rightarrow CH_3OH + Y^-$ Product Energy Partitioning.

	f_{rot}'	f_{vib}'	f_{int}'	f_{rel}'
		$OH^- + CH_3Cl \rightarrow CH_3OH + Cl^-$		
Direct rebound	0.03 ± 0.01	0.62 ± 0.02	0.65 ± 0.02	0.35 ± 0.02
Direct stripping	0.04 ± 0.01	0.69 ± 0.04	0.73 ± 0.04	0.27 ± 0.04
Indirect	0.08 ± 0.01	0.78 ± 0.01	0.87 ± 0.01	0.13 ± 0.01
Total	0.07 ± 0.01	0.74 ± 0.01	0.81 ± 0.01	0.19 ± 0.01
		[a]$OH^- + CH_3I \rightarrow CH_3OH + I^-$		
Direct rebound	0.16 ± 0.01	0.63 ± 0.01	0.79 ± 0.01	0.21 ± 0.01
Direct stripping	0.07 ± 0.01	0.66 ± 0.01	0.73 ± 0.01	0.27 ± 0.01
Indirect	0.09 ± 0.01	0.77 ± 0.01	0.86 ± 0.01	0.14 ± 0.01
Total	0.10 ± 0.01	0.70 ± 0.01	0.80 ± 0.01	0.20 ± 0.01

[a] the fractions of the product energy partitioning for the $OH^- + CH_3I$ reaction in ref 9;

Table S3. The reaction probabilities and rate constant for the OH^- + CH_3Y (Y = Cl, I) Reaction Pathways.

	systems	
reaction probability	OH^- + CH_3Cl	OH^- + CH_3I[a]
total reaction	0.35 ± 0.03	0.42 ± 0.03
$CH_3OH + Y^-$	0.35 ± 0.03	0.23 ± 0.02
$CH_2Y^- + H_2O$	—	0.18 ± 0.02
$[CH_3\text{--}Y\text{--}OH]^-$	—	0.01 ± 0.01
rate constant [b, c]	$(1.3\text{-}1.6) \times 10^{-9}$	1.7×10^{-9}

[a] The reaction probability for the OH^- + CH_3I reaction at the B97-1/ECP/d level of theory at E_{coll} = 0.04 eV reported in ref 10. [b, c] The experimental rate constant ($cm^3 \cdot mol^{-1} \cdot s^{-1}$) for the OH^- + CH_3Cl and OH^- + CH_3I reactions reported in ref 20, 22, 25 and 10, respectively.

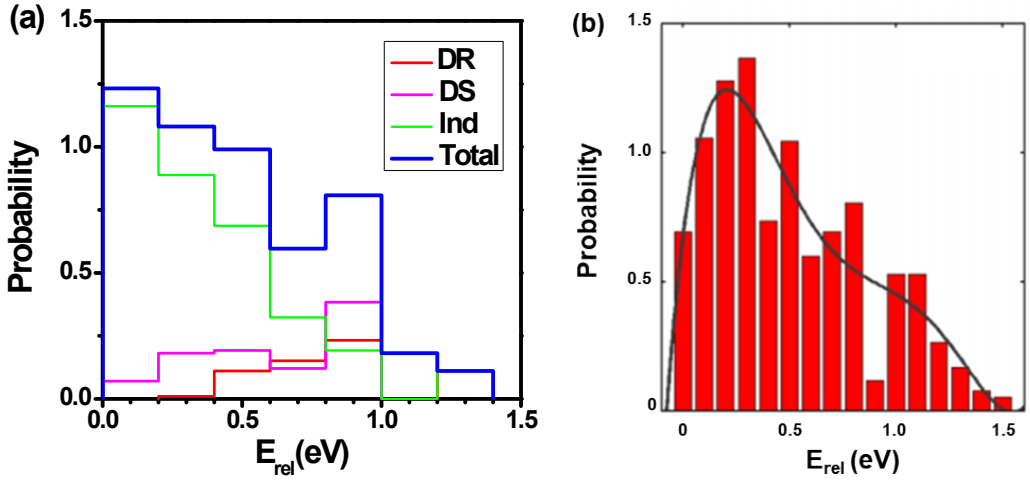

Figure S2. (a) the product relative translational energy distributions for the OH^- + CH_3Cl reaction at the B3LYP/aug-cc-pVDZ level of theory at E_{coll} = 0.04 eV. Results are presented for the direct rebound (red), the direct stripping (purple), and the indirect (green) atomic-level mechanisms, as well as for the total reaction (blue); (b) the product relative translational energy distributions for the OH^- + CH_3I reaction at the B97-1/ECP/d level of theory at E_{coll} = 0.05 eV reported in ref 9.

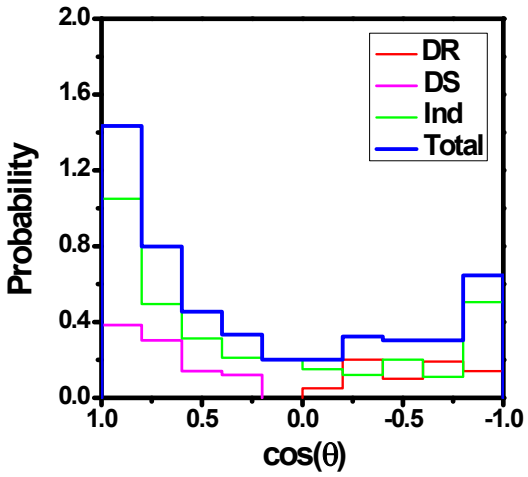

Figure S3. Histogram of the velocity scattering angle distribution for the $OH^- + CH_3Cl$ reaction at the B3LYP/aug-cc-pVDZ level of theory. Results are presented for the direct rebound (red), the direct stripping (purple), and the indirect (green) atomic-level mechanisms, as well as for the total scattering (blue).

Supplementary movies:

Representative trajectories of (1) DR mechanism, (2) DS mechanism, (3) Ind-pre mechanism, (4) Ind-pre+PE mechanism, (5) Ind-pre+PE+BR mechanism, as well as (6) Ind-pre+post mechanism, and (7) Ind-pre+post+PE mechanism at E_{coll} = 0.89 kcal mol^{-1} for the $OH^- + CH_3Cl$ reaction.